IDENTIFICATION OF VISCOELASTIC MODULI OF COMPOSITE MATERIALS FROM THE PLATE TRANSMISSION COEFFICIENTS

Bernard Hosten and Michel Castaings
Laboratoire de Mecanique Physique, University of Bordeaux I, URA
C.N.R.S. No.867
351, Cours de la Liberation, 33405-Talence Cedex, France

Tribikram Kundu
Department of Civil Engineering and Engineering Mechanics
University of Arizona, Tucson, Arizona 85721, USA

INTRODUCTION

A quick and accurate method of measuring elastic and viscoelastic constants of a material is the essential first step for characterizing the material. This is more challenging for composite materials because unlike homogeneous metals and ceramics the material properties change from specimen to specimen for composite materials as the volume fraction of fibers and their orientations change. Anisotropic properties of composite materials add another difficulty in the measurement technique, since anisotropy increases the number of independent material constants. Polymer composites exhibit a high degree of attenuation in the matrix material; as a result, these composite materials cannot be assumed to be pure elastic material, so they should be modeled as viscoelastic materials by making the material constants complex. The real part is associated with the elastic behavior and the imaginary part is associated with the viscoelastic or attenuative behavior of the material. The number of independent material constants for a unidirectional (UD) composite, which is transversely isotropic, is ten (five real and five imaginary). Naturally, it is not practical and almost impossible to measure all these material constants by the traditional engineering method of applying stresses and measuring strains in different directions. Because of the measurement difficulty the imaginary parts of the material constants are often ignored. However, it should be mentioned here that it is important to measure the imaginary components of material constants because porosity and microcracking in the matrix due to material fatigue and aging affect the attenuation more than the elastic properties. In other words, the imaginary components of the material constants are a better indicator of material aging compared to the real components. Hence, an efficient technique to measure both real and imaginary components of the material constants is warranted and developed in this paper.

Review of Progress in Quantitative Nondestructive Evaluation, Vol. 17
Edited by D.O. Thompson and D.E. Chimenti,, Plenum Press, New York, 1998

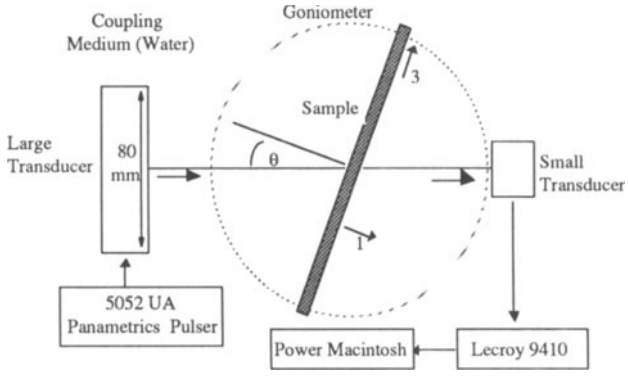

Figure 1. Experimental setup for bulk wave and transfer function techniques for material characterization.

BACKGROUND

In recent years, during the last two decades, several investigators attempted to measure material properties of composites by propagating bulk or body waves and Lamb waves through a composite plate. Rokhlin and his associates [1-3], as well as Hosten and his co-investigators [4-5] propagated bulk waves through the plate for this purpose. It is possible to propagate quasi-longitudinal (QL) and quasi-transverse (QT) bulk waves through a plate by simply rotating the plate with respect to the transmitting and receiving transducers by a goniometer, as shown in Fig. 1.

The angle of incidence (θ in Fig. 1) of the ultrasonic beam changes as the plate is rotated. In this manner simply by changing θ both QL- and QT-waves can be generated and propagated in different directions of the plate. At normal incidence only the longitudinal wave is generated. For an incident angle greater than the QL critical angle but less than the QT critical angle, only the QT waves are generated. For the non zero angle of incidence that is less than the QL critical angle, both QL and QT waves are generated. From the difference in the arrival times, QL and QT modes can be separated. In this manner slowness values (inverse of the wave velocity) in different directions of the plate can be experimentally measured. The imaginary parts of the slowness vector are deduced from the attenuation measurements [4-5]. Material properties can be obtained from these curves by solving the inverse problem. One difficulty with this approach is that it is not possible to experimentally obtain the wave speed of both QL and QT modes for all angles. They are generated for only limited regions and then extrapolated. This extrapolation may give error for large incident angles, for which no experimental values are present.

This method works only when the plate thickness is larger than the wave length and the QL and QT echoes can be separated. One way to separate these two modes is to increase the signal frequency. However, if the frequency is too high then plies and fibers in a composite material scatter away the signal and the plate no longer appears to be homogeneous.

Mal and his associates [6-7] measured material properties by inverting the leaky Lamb wave dispersion curves. It is possible to measure elastic properties in this manner; however, this method is not efficient for measuring the viscoelastic properties because the phase velocity dispersion curves are not sensitive enough to the material viscoelasticity.

TRANSFER FUNCTION METHOD

The above mentioned difficulties associated with the experimental measurements of the complex material properties can be eliminated by the transfer function method. In this technique the entire transmitted waveform received by the receiving transducer is compared to the theoretical values in the frequency domain. The transfer function or the transmission coefficient as a function of the frequency for different incident angles, is then inverted by the simplex algorithm for obtaining the material properties. In this technique the separation of QL and QT modes in the time domain is not necessary, hence the plate can be thin compared to the signal wave length. Kinra and his associates [8-10] measured thickness and wave speeds in isotropic thin plates by the transfer function method for normal incidence. In this paper oblique incidence is also considered and both elastic and viscoelastic constants of a unidirectional (UD) glass fiber reinforced polymer composite plate are obtained.

EXPERIMENTS AND RESULTS

The experimental setup is shown in Figure 1. A large transducer is used for generating the signal with a plane wave front. The transducer was manufactured by Imasonic. It has a center frequency of 3.2 MHz with 20 dB down points at 2 and 5 MHz and an 80 mm x 40 mm rectangular front face, the longer axis being aligned parallel to the plane of the wave propagation (see Fig. 1). Then the length of the transducer is equal to 170 wavelengths in water (the coupling medium) at the center frequency, giving a good approximation to plane wave conditions [11]. The small transducer on the receiving side is a Panametrics transducer (U302) that has a central frequency of 1 MHz. This arrangement was chosen so that we can measure the material properties at a lower frequency range (0.5 - 1.5 MHz), although the central frequency of the large transducer is much higher. In this manner simply by changing the receiving transducer (which is less expensive because it is smaller and commercially readily available) material properties can be determined for different frequencies. Since in this case the generated wave front is a plane wave front, detecting it by a smaller transducer does not significantly alter the plane wave condition.

The stress-strain relation for the transversely isotropic and orthotropic solids is given by:

$$\begin{Bmatrix} \sigma_{11} \\ \sigma_{22} \\ \sigma_{33} \\ \sigma_{12} \\ \sigma_{13} \\ \sigma_{23} \end{Bmatrix} = \begin{bmatrix} C_{11} & C_{12} & C_{13} & 0 & 0 & 0 \\ & C_{22} & C_{23} & 0 & 0 & 0 \\ & & C_{33} & 0 & 0 & 0 \\ & & & C_{44} & 0 & 0 \\ & \text{Symm} & & & C_{55} & 0 \\ & & & & & C_{66} \end{bmatrix} \begin{Bmatrix} \varepsilon_{11} \\ \varepsilon_{22} \\ \varepsilon_{33} \\ \varepsilon_{12} \\ \varepsilon_{13} \\ \varepsilon_{23} \end{Bmatrix}. \tag{1}$$

The material constants C_{ij} are complex if the material has attenuation.

$$C_{ij} = C'_{ij} + iC''_{ij} \tag{2}$$

The real and imaginary components C'_{ij} and C''_{ij} are associated with elasticity and viscoelasticity of the material, respectively.

The reference coordinate system is chosen such that the x_1 axis is normal to the plate surface and the x_3 direction is aligned with the fiber direction (see Fig. 1). This preliminary study emphasizes the measurement of material properties in the x_1x_3 anisotropic plane. The plate is rotated by the goniometer around the x_2 axis in steps of few degrees while taking readings.

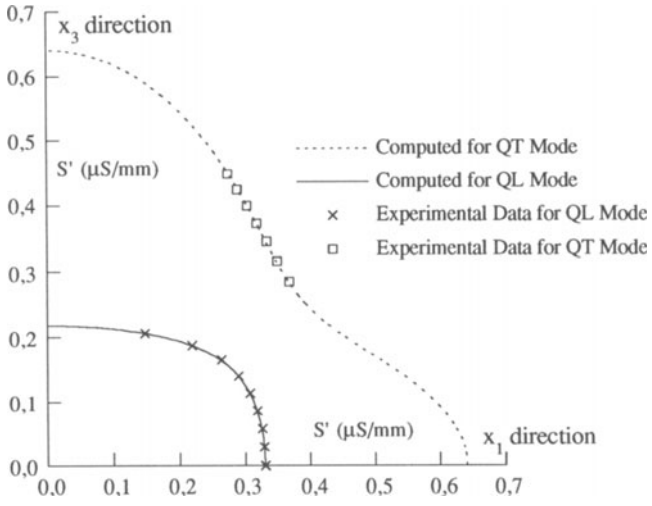

Figure 2. Slowness variation as a function of the direction of propagation in the composite plate specimen for QL mode (solid line) and QT mode (dashed line).

A glass fiber reinforced composite plate of thickness 5.73 mm and 1.80 gm/cc density is taken for the experiment. Wave speeds inside this specimen along different directions in the x_1x_3 plane are obtained from the phase difference [12] between the frequency spectra of the reference signal (received signal in absence of the plate) and the received signal for different inclined positions of the plate between the two transducers. The slowness (inverse of the wave speed) for the QL and QT modes are plotted in polar coordinates in Figure 2. Horizontal and vertical axes of this figure represent x_1 and x_3 directions respectively. Experimentally obtained slowness values for QL and QT modes are shown by cross and square markers respectively. Two curves are fitted through these experimental values by optimizing the material moduli by the Newton-Raphson technique. For the optimized values, given in Table 1, the computed curves for the QL and QT modes pass through the experimental points without any visible difference between the experimental points and the computed curve.

In Table 1 C_{bij} and C_{tij} represent material properties obtained by the bulk wave technique, discussed above, and the transfer function technique, discussion follows, respectively.

For measuring the material properties by the transfer function method the experimental setup does not change. In this case, the entire signal received by the receiver is recorded. The transfer function (frequency spectrum of the received signal divided by that of the reference signal which is obtained in absence of the plate) for different inclinations of the plate are recorded. Experimental transfer functions for 0°, 10° and 30° incident angles are shown by cross markers in top, middle and bottom graphs of Fig. 3.

OPTIMIZATION BY THE SIMPLEX ALGORITHM

The material properties (C_{tij}) are optimized by the simplex algorithm [6,13-16]. For

this purpose an error function is first defined in the following manner

$$E = \sum_{v=1}^{p} \sum_{u=1}^{q} (v_{cuv} - v_{euv})^2 \qquad (3)$$

where v_{cuv} is the modulus of the computed transmission coefficient at frequency f_u and angle of incidence θ_v for an assumed set of material parameters and v_{euv} is the experimental value for the same frequency and angle of incidence.

Table 1. Computed material constants in GPa by bulk wave and transfer function techniques

C_{ij} & Method	C_{11}'	C_{33}'	C_{55}'	C_{13}'	C_{11}''	C_{33}''	C_{55}''	C_{13}''
Bulk (C_{bij})	16.4	37.9	4.4	7.2	0.8	0.9	0.2	0.2
Transfer (C_{tij})	16.6	37.3	4.4	7.3	0.7	1.4	0.2	0.4

For m number of unknown material parameters the simplex algorithm starts with (m+1) number of initial guesses of the material parameters, C_{tij}. Every initial guess constitutes a vertex of the simplex geometry. The simplex algorithm computes error from Eq.(3) for every vertex point of the simplex. Then it replaces the worst vertex that is associated with the maximum error by a new vertex (a new set of material parameters), by one of the four operations - reflection, expansion, contraction or shrinkage [13-16]. Systematically carrying out these steps it converges to a point which gives minimum error. This technique completely avoids the need for numerical differentiation and matrix operation. As a result, computationally it is very fast compared with the conventional techniques, such as the Newton-Raphson technique. It always converges to some minimum error point. However, the point of convergence can be a local minimum (not the point of one's interest) or a global or absolute minimum (the point of interest). If one starts with a good set of initial guesses, not very far from the true values, then it should converge to the absolute minimum, otherwise it may converge to a local minimum point. The probability of converging to the absolute minimum increases as the number of unknown parameters decreases.

To keep the number of unknown material parameters small, we first optimize C_{t11} from the transfer function for the normal incidence. Normal incidence is not affected by other material parameters. In this step of optimization only two unknown material parameters, the real and imaginary components of C_{t11}, are obtained. They were optimized by taking 52 frequency points between 0.5 and 1.5 MHz frequency. Except for one point near 0.5 MHz the matching between the computed transfer function (solid line) and the experimental points (crosses) in Figure 3 is excellent in this region. The converged values of C_{11}' and C_{11}'' (16.6 and 0.7, shown in Table 1) when compared with the bulk mode predicted values (16.4 and 0.8), show that the real part converged very well, but the imaginary part has 12.5% difference. To see which of these predictions is the best, the transfer function computed with C_{bij} are also plotted by dashed lines in Figure 3. Both predictions fit the experimental data for the normal incidence. However, the transfer function method seems slightly better. The matching is bad above 2 MHz because this region is beyond the small transducer bandwidth and the experimental data cannot be fully trusted. Since both computed transfer functions matched the experimental data well in spite of 12.5% difference in the C_{11}'' one can conclude that the transfer function is not as sensitive to the imaginary part as it is to the real part of C_{11}. That is why the real part matched better than the imaginary part. However, if we completely ignore the imaginary part then the experimental data cannot be matched with the theoretical curves very well. Hence, it is important to take into account the effect of the material attenuation.

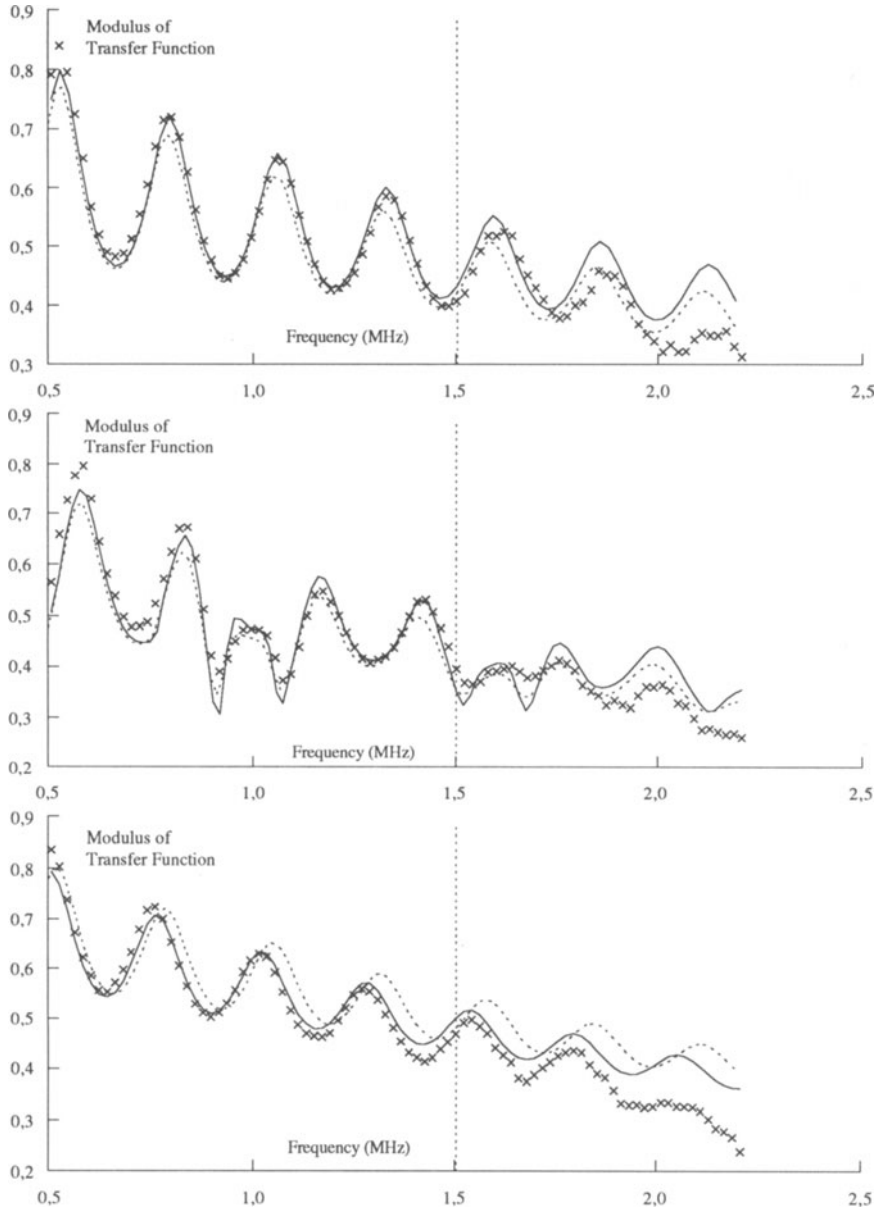

Figure 3. Transfer functions for 0° (top), 10° (middle) and 30° (bottom) angles of incidence. Experimental data between 0.5 and 1.5 MHz (left of the vertical dotted line) are taken for the simplex optimization.
x : Experimental Data ; Solid Line : Computed from C_{ij} ; Dashed Line Computed from C_{bij}

The other three complex material constants in the x_1x_3 plane must be considered simultaneously. For six real unknown parameters, one needs to have a very good estimate of the material parameters for converging to the correct values by the simplex algorithm. To avoid this difficulty associated with a large number of unknown parameters we first treated three imaginary components as known values, and assigned some small values to those and

considered only the three real components as the unknown parameters. The simplex algorithm does not have much difficulty to optimize only three parameters. To check whether it converged to a local or absolute minimum, the optimization is carried out with different perturbations (about 40%) or initial guesses. If the convergence points are same then it is concluded that it converged to the absolute minimum. After obtaining the real constants, the three imaginary constants are optimized. The real and imaginary constants thus obtained should be very close to the correct values. Next, this process of optimizing three real constants and three imaginary constants can be continued for a few times until the final convergence is achieved (typically it takes one or two additional iterations), alternately all six constants can be optimized at the same time after a good estimate of their values are obtained from the first iteration. The final converged values of C_{t33}, C_{t55} and C_{t13} are given in Table 1. Again one can see good matching between the real components predicted by the two techniques but a significant amount of scatter in the imaginary components.

Transfer functions plotted for 10° and 30° incident angles in Figure 3 show very good matching between the experimental and theoretical values in the 0.5 - 1.5 MHz region used for the simplex inversion. A careful observation reveals that the matching between the solid line and the experimental points appears to be somewhat better than that between the dotted line and the experimental points. This suggests that the correct values are probably closer to the C_{tij} than C_{bij}. One can also notice in the transfer functions that experimental values appear to be more attenuated beyond 1.5 MHz compared to the predicted values, and matching becomes worse. This is due to the fact that the material properties, specially the imaginary components are not completely frequency independent, as we are assuming. As a result, theoretical predictions do not match the experimental data for all frequency ranges equally well.

The difference between the experimental and predicted waveforms are comparatively less prominent. Figure 4 shows the received waveform for the 10° incident angle. Computed waveforms from both C_{tij} and C_{bij} values look identical and vary only slightly from the experimental values. Hence, it is better to compute the material parameters by minimizing the error computed from the mismatch of the transfer functions, as done in this paper, than from the mismatch of the waveform.

CONCLUDING REMARKS

A new method based on the transfer functions of plates is used in this paper for identifying the material properties of viscoelastic anisotropic materials. A comparison between the material properties predicted by the bulk wave technique and by the transfer function technique shows that real components (elastic properties) can be accurately predicted by both techniques. However, the prediction of the imaginary components are not as accurate as the real components. In a relative scale between these two techniques, the transfer function technique appears to be more reliable for predicting the viscous properties. This can be justified from the fact that the transfer function technique works with the complete transmitted waveform and the bulk wave technique works with the amplitude and the first arrival of the QL and QT modes only. As a result more information is taken into account during the signal processing when the transfer function technique is followed. More work has to be done te estimate the C_{ij} precision.

As mentioned before, for the bulk wave technique the separation of QL and QT echoes is essential, but that is not necessary for the transfer function technique. Hence, one can work at a relatively low frequency and characterize thin plates when the transfer function technique is applied. The bulk mode technique is very sensitive to the fluctuation of the coupling medium properties (temperature gradient , etc...), because it takes into account also the propagation times of QL and QT pulses in this medium. At the opposite, the transfer function technique is only sensitive to what happens inside the plate.

ACKNOWLEDGMENT

Part of this work was carried out during a visit by Tribikram Kundu to the Bordeaux IUniversity funded by the University.

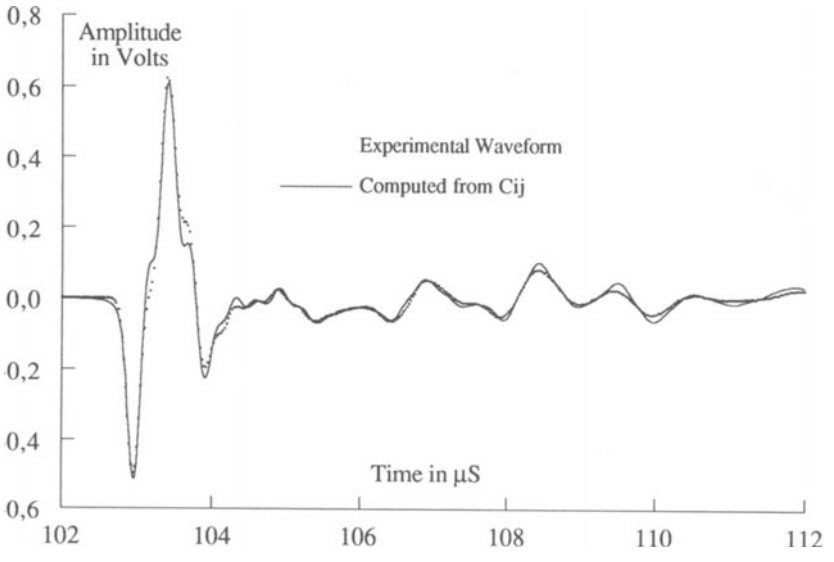

Figure 4. Received waveform for the 10° angle of incidence.

REFERENCES

1. S. I. Rokhlin, and W. Wang, J.Acoust.Soc.Am. 91, 3303-3312 (1993).
2. S. I. Rokhlin, and W. Wang, J.Acoust.Soc.Am. 94, 2721-2730 (1994).
3. Y. C. Chu, and S. I. Rokhlin, J.Acoust.Soc.Am. 95, 3204-3212 (1994).
4. B. Hosten, M. Deschamps, and B. R. Tittmann, J. Acoust. Soc. Am., 82, 1763-1770 (1987).
5. B. Hosten, J. Acous. Soc. Am. **89**, 2745-2752 (1991).
6. M.R. Karim, A.K. Mal and Y. Bar-Cohen, J.Acoust.Soc.Am. 88, 482-491 (1990).
7. A.K. Mal, S.S. Lih and Y. Bar-Cohen, Review of Progress in Quantitative NDE, Vol 13, DO Thompson and DE Chimenti (eds), Plenum Press, New York, pp1149-1156 (1994).
8. V. K. Kinra, C. Zhu, J. Acoust. Soc. Am Vol. 93, 2454-2467 (1993).
9. V.K. Kinra, V.R. Iyer, Ultrasonics, 33, 95-109, (1995).
10. V.K. Kinra, V.R. Iyer, Ultrasonics, 33, 111-122, (1995).
11. P. Cawley, and B. Hosten, J. Acoust. Soc. Am., 101(3), 1373-1379, (1997).
12. W. Sachse, and Y. H. Pao, Journal of Applied Physics, Vol.49, pp.4320-4327, 1978.
13. J. A. Nelder and R. Mead, Computer Journal, Vol.7, p.308-315, 1965.
14. M. S. Cacei and W. P. Cacheris, Byte, pp.340-362, 1984.
15. T. Kundu, J. Acoust. Soc. Am., Vol.91, pp.591-600, 1992.
16. T. Kundu, J. Bereiter-Hahn, and K. Hillmann, Biophysical Journal, Vol.59, pp.1194-1207, 1991.